shielding walls will be ~1-m thick, and the transverse walls will be ~1.5-m thick. Polyethylene will be used to shield neutrons, and additional lead and/or steel will be used for localized shielding as needed. An alternative shielding implementation that will be considered in the future is to replace some of the excavated earth to provide some fraction of radiation shielding. Earth has a density that is ~70% that of heavy concrete, so ~7 ft of earth would provide the equivalent of 5 ft of concrete shielding.   Much further analysis is required from the Radiation Physics Department to establish actual shielding requirements.

Further analysis is needed to determine if the concrete tunnel floor in the DBA arcs needs to be rebuilt for additional stability. A significant engineering task is to determine how or if the accelerator floor will connect with the experimental hall floor to achieve maximum stability of each beam line with respect to the electron orbit in the associated photon source magnet.

The accelerator tunnel in the four TME arcs may require refurbishment to control water seepage and other imperfections.

4.1.14 Facility Preservation

The successful reuse of equipment from PEP-II will depend on proper maintenance over the next decade. Vacuum chambers will be vented to dry nitrogen, water cooling channels for vacuum chambers and magnet conductors will be drained and blown dry, and a program of preventive maintenance and/or safe storage will be instigated for all components of value, including power supplies, instrumentation and control components, utility infrastructure and other accelerator components.

4.2 Photon Beam Line Systems

The preservation of photon beam emittance, coherence and stability in the presence of the unprecedented beam power of PEP-X poses a significant challenge for beam line design. While it is reasonable to assume improvements relative to the current state of the art of beam line component and optics technology, this report outlines a conservative, proof of principle beam line design respecting the constraints imposed by existing technology. Consequently, preliminary beam line layouts utilize long drift lengths to reduce power densities to manageable levels and aggressive beam aperturing and filtering to minimize the power deposited in key optical components. Nonetheless, optics designs based on current technology cannot preserve fully the extraordinary emittance of the PEP-X source. Emittance preservation is likely to be enhanced as x-ray optics technology evolves.

4.2.1   High Power Beam Lines

As detailed in Table 3.1.2, the U23 undulator develops the greatest power density of the representative ID sources. Power density represents a key constraint in beam line design as it defines the minimum distance between source and first power masks. As demonstrated shortly, once properly apertured and filtered, the optics can manage the remaining thermal load with relatively modest power-induced degradation of the beam emittance. The higher total power though lower power density of the longer period ID, such as W50, alter the beam line design problem. These inherently lower-brightness ID beam lines reduce the emphasis on emittance preservation, but the optics must cope with greater total power to extract the maximum performance from the source. Since these sources represent a minority application on a low emittance ring such as PEP-X and a successful undulator beam line design solution can be

applied to a wiggler by reducing the beam line acceptance (at the price of reduced flux), our proof-of-principle design focuses on a U23 undulator beam line.

The peak power density of U23 with PEP-X at 4.5 GeV/1.5 A is 1038 kW/mrad^2 at k_{max} as listed in Table 3.1.2. Typically, intensively water-cooled Glidcop masks can tolerate 5-10 W/mm^2 steady state power deposition over large areas where the larger value can be sustained only if the mask surface can be profiled to expand the power footprint (e.g., a "crenelated" mask surface divides the power footprint into displaced alternating power stripes, resulting in a lower surface average power density). If one assumes the smaller 5 W/mm^2 limit and a 0.75°-1.0° beam incident angle, then the first masks that intercept the U23 peak power density must be at least 52-60 m from the source. Figure 4.2.1 plots the U23 beam horizontal and vertical power density variation with observation angle. At 60m from the source the beam half width at 10% power density is 16.5 mm horizontal by 9.0 mm vertical. Assuming rather stringent ±0.1 mrad beam steering tolerance increases this 10% power density half envelope to 22.5 mm by 15.0 mm. At 1.0° incident angle 1.3 m of mask is required to intercept 22.5 mm of beam. This is technologically feasible, particularly if distributed over several mask assemblies.

It should be noted that a ±0.1 mrad maximum steering envelope does not provide much steering tolerance for stored beam configuration development. The steering tolerance can be expanded at reduced stored current by employing larger acceptance, thermally de-rated masks upstream of the full power rated front end components. These de-rated masks could consist of relatively low-cost refractory metal collimators with thermal sensors for machine protection and/or short water-cooled Glidcop masks with steeper beam intercept angles.
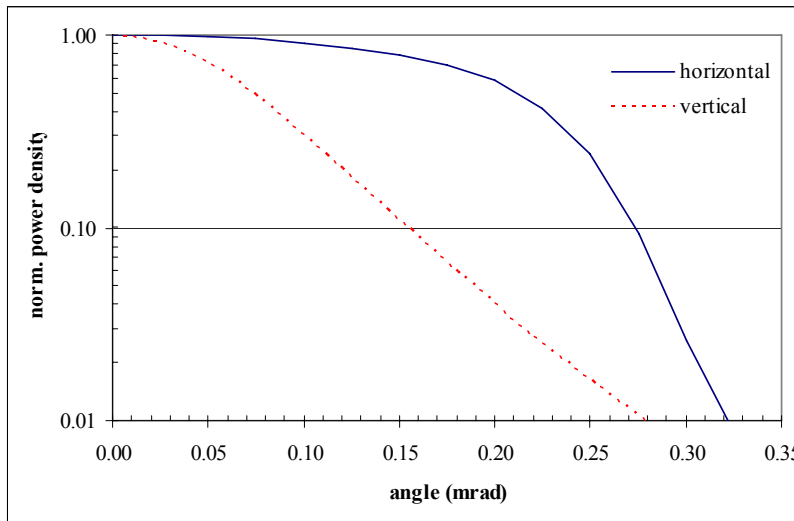

Figure 4.2.1: The U23 normalized power density at k_{max} as a function of horizontal and vertical observation angle for the ring and undulator parameters tabulated in Section 3.1.

It is advantageous to intercept and discard as much waste power in the front end masks as possible in order to minimize the power on downstream masks and optics. Utilizing apertures to limit the beam line acceptance to $3\sigma'$, where σ' is the effective rms angular width of the undulator central cone, transmits almost 90% of the central cone flux. The undulator effective central-cone opening angle as a function of photon energy is listed in Table 4.2.1. Inspection of this table indicates a 30 µrad by 30 µrad acceptance is adequate for a broad range of x-ray energies. For higher energy applications a more restrictive 20 µrad by 20 µrad acceptance is sufficient. Figure

4.2.2 plots the transmitted power as a function of rectangular pinhole acceptance. The total power transmitted by a 30 μrad by 30 μrad pinhole is 925 W whereas the 20 μrad by 20 μrad pinhole transmits only 420 W. As discussed in Section 4.2.3, 925 W exceeds the power rating of LN-cooled silicon monochromators.

Table 4.2.1: U23 undulator emission envelope as a function of photon energy. The photon beam effective rms opening angle $\sigma_{x'\_eff}$ ($\sigma_{y'\_eff}$) is the quadrature sum of the electron beam $\sigma_{x'}$ ($\sigma_{y'}$) listed in Table 3.1.1 and the diffraction limited photon opening angle $\sqrt{(\lambda/L)}$ where L=3.5m.

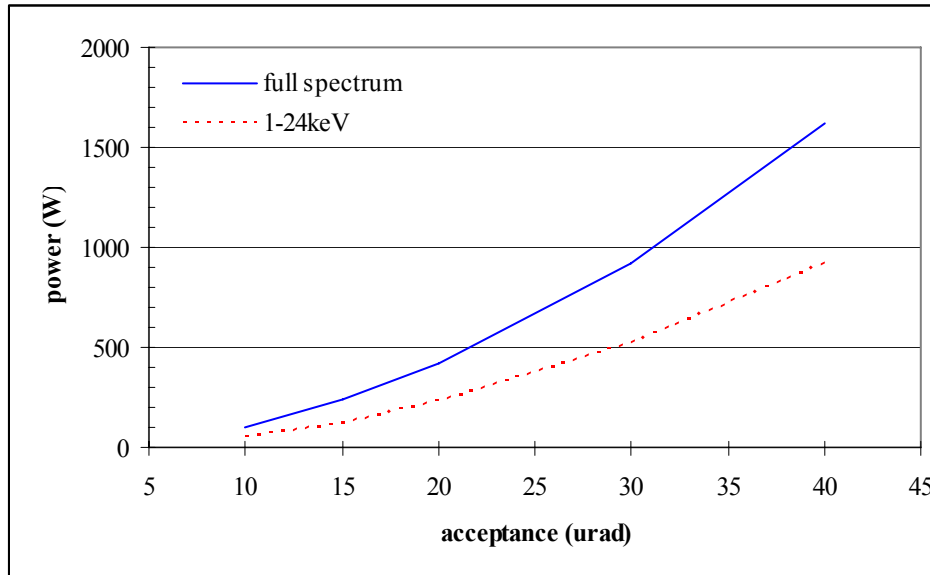| E (keV)	$\sigma_{x'\_eff}$ (μrad)	$\sigma_{y'\_eff}$ (μrad)	$3\sigma_{x'\_eff}$ x $3\sigma_{y'\_eff}$
5.0	9.3	8.5	27.9 x 25.5
10.0	7.2	6.0	21.6 x 18.0
20.0	5.8	4.3	17.4 x 12.9
40.0	5.0	3.1	15.0 x 9.3

Figure 4.2.2: U23 power at k_{max} transmitted through a rectangular pinhole acceptance for 4.5GeV/1.5A. The solid blue line is integrated over the entire emission spectrum whereas the dashed red line is integrated up to 24 keV as an approximation to the power obtained downstream of a low pass filter mirror.

4.2.2   Mirrors

Introducing a flat mirror in the beam line provides needed power filtering. For example, a Rh-coated mirror operating at 2.7-mrad incident angle cuts off the transmitted spectra for energies greater than the 23.2 keV Rh k-edge. Integrating the beam transmitted through a 30-μrad pinhole up to 24 keV shows that such a mirror reduces the downstream power to 520 W. The remaining 405 W is deposited in the mirror at an average power density of approximately 0.3 W/mm^2 which does not present a significant thermal deformation concern. Finite element analyses of water-cooled silicon mirrors with cross-sections designed to minimize thermal distortion indicate

the thermal figure distortion is less than 0.7 µrad rms for a more demanding 0.5 W/mm^2 and 600-W absorbed power load. (<0.1µrad rms for 0.12W/mm^2 and 140W). Though a more expensive approach, cryogenically-cooled silicon mirrors would eliminate thermal distortion as a source of emittance degradation. While the thermal deformation is not cause for excessive concern, introduction of a mirror can degrade the beam characteristics as addressed in more detail below. Long wavelength figure error can be corrected actively using adaptive mirror technology, but shorter wavelength errors will contribute to emittance and coherence degradation. Since the source horizontal emittance is much larger than the vertical emittance, the beam degradation is less problematic for a horizontally deflecting mirror than a vertically deflecting mirror. A horizontally deflecting mirror is also less subject to gravitational induced figure deformation. The long optical lever arm associated with a mirror located at approximately 65 m (i.e., inside the storage ring concrete shielding) imposes mirror stability requirements that will necessitate active mirror pointing feedback as is practiced at most third generation synchrotron sources.

The 520W transmitted by a 30-µrad pinhole coupled with a 24-keV low pass mirror still exceeds the power that can be managed with existing cryogenically-cooled monochromators without introducing observable crystal thermal distortion. More aggressive aperturing. transmitting only a $3\sigma_{x'eff}$ x $3\sigma_{y'eff}$ beam, helps at higher photon energies but at low energies more effective power filtering is required. For a beam line designed for only low energy applications, a fixed, low-energy cutoff mirror can be used. More generally, a variable cutoff energy mirror system can be devised using two anti-parallel mirrors with variable angle of incidence. By employing an anti-parallel or periscope-like mirror system geometry, the axis of the downstream optics can be fixed independently of the mirror system cutoff energy. Reducing the acceptance to $3\sigma_{x'eff}$ x $3\sigma_{y'eff}$ and employing a variable cutoff mirror system significantly reduces the power transmitted to the monochromator as illustrated in Figure 4.2.3.
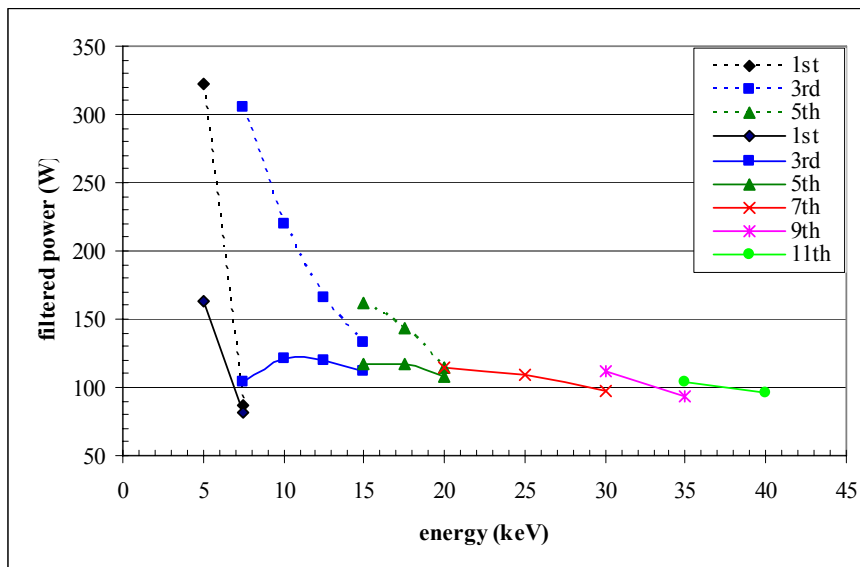

Figure 4.2.3: Transmitted power of U23 along odd harmonic tuning curves with a $3\sigma_{x'eff}$ x $3\sigma_{y'eff}$ aperture and low-pass mirror filtering. The broken lines depict the results for a fixed 24-keV cutoff energy mirror system while the solid lines depict the results for a variable cutoff mirror system adjusted to filter harmonics higher then the specified harmonic.

Introducing a cutoff mirror inside the storage ring offers several side benefits besides power filtering. The suppression of the higher energy portion of the synchrotron spectra and the displacement of the pink synchrotron beam out of the gas Bremsstrahlung cone greatly simplifies beam line shielding. Additionally, the mirror body becomes a source of Compton scatter that can

be monitored to provide vertical beam position information for electron beam steering feedback. This approach, which has been employed successfully on an SSRL undulator beam line, has the virtue of utilizing the core of the undulator beam and minimizing contamination from bend magnet radiation.

4.2.3 Monochromators

Aggressive aperturing and power filtering, as depicted in Figure 4.2.3, limits the power transmitted to the monochromator to 90-125W typical and 165W maximum. Assuming the monochromator is located at 78 m near the downstream end of the FOE, 7-15 W/mm^2 power density is incident on the monochromator first crystal surface for photon energies 5-20 keV with a Si(111) crystal, or 9-16.5 W/mm^2 for 7-40 keV with a Si(220) crystal. The power density variation with tuning and crystal index is shown in Figure 4.2.4. Relocating the monochromator downstream closer to the experimental hutch (~110 m) reduces the power density up to two-fold, but it increases shielding complexity owing to the transport of pink beam from the FOE.
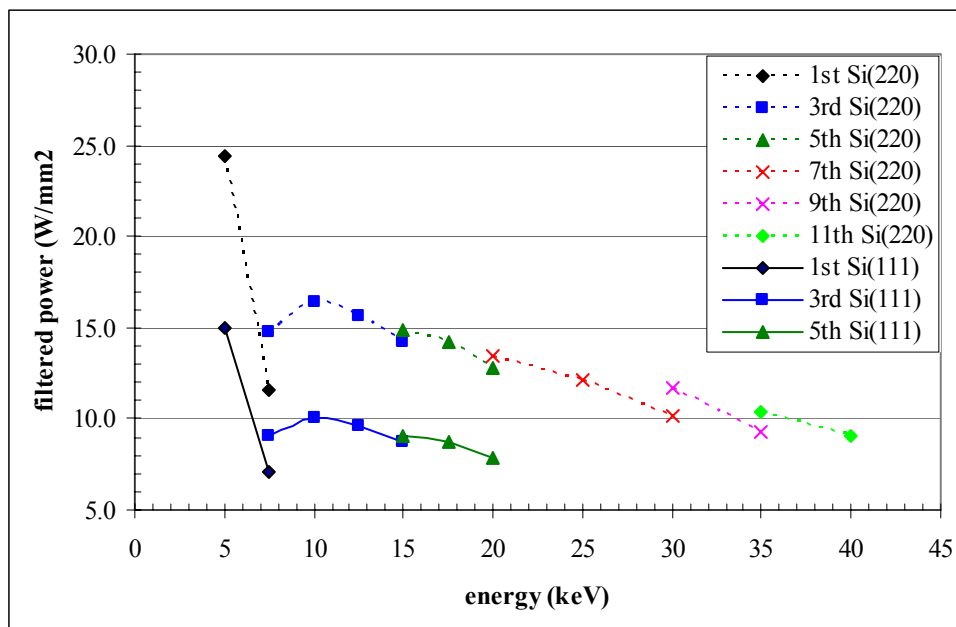

Figure 4.2.4: Power density incident on a U23 monochromator first crystal surface along odd harmonic tuning curves assuming a $3\sigma_{x'eff}$ x $3\sigma_{y'eff}$ aperture and a variable cutoff mirror system adjusted to filter harmonics higher then the specified harmonic. The broken lines represent the power density for a Si(220) crystal while the solid lines depict similar results for a Si(111) crystal.

Cryogenically-cooled monochromator crystals are used extensively on high-power density beam lines at third generation light sources, including SSRL. The internally LN-cooled Si crystals employed in the SSRL LN monochromator have been studied extensively through finite element analysis (FEA) as well as empirically under 500-mA SPEAR3 beam conditions. In particular, the response of these crystals has been calculated for 200-W applied beam power and 8-11 W/mm^2 power footprint geometries similar to that of a PEP-X monochromator. The thermal analyses indicate 95-101 K maximum surface temperatures and 2.3-3.2 μrad rms thermal deformation. The temperature profile of the 11.1 W/mm^2 case is depicted in Figure 4.2.5. The results of the FEA clearly demonstrate that monochromator thermal performance requires improvement in order to preserve the PEP-X emittance. Possible fruitful areas for investigation include improved crystal materials (e.g., isotopically pure diamond) and enhanced cryogenic cooling of silicon whereby the crystal is maintained in a more isothermal state at a temperature closer to that of zero thermal expansion (i.e., ~130 K). It should be noted that SPEAR3 operating at 500 mA

provides a very good platform for monochromator research as "improperly" filtered beams from various SPEAR3 IDs can attain the powers and power densities of Figures 4.2.3 and 4.2.4.
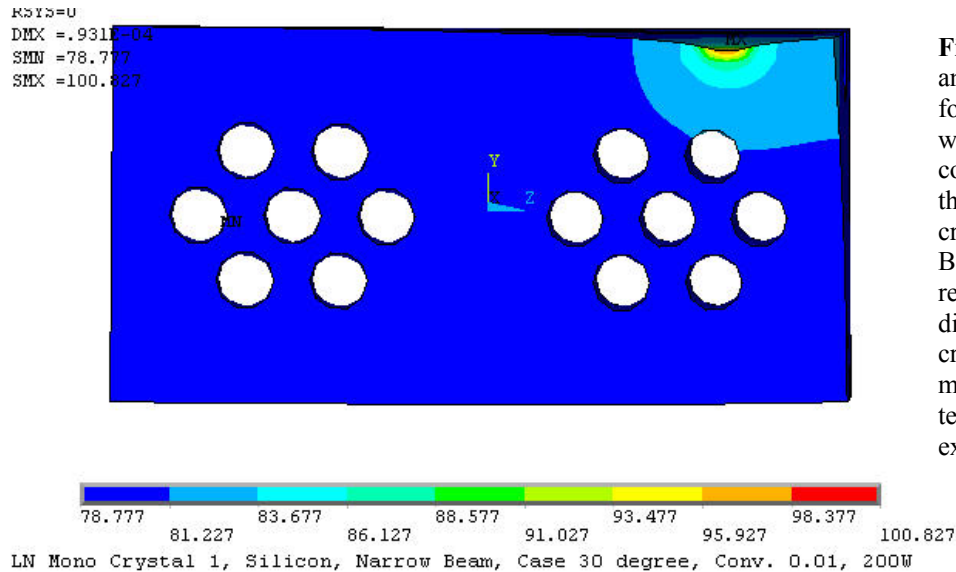

Figure 4.2.5: FEA of 200-W and 11.1-W/mm^2 power footprint on a silicon crystal with liquid nitrogen internal cooling. The calculated thermal distortion of the crystal is 3.17 µrad rms. Both empirical and FEA results indicate that the distortion is reduced if the crystal temperature is maintained closer to the temperature of zero thermal expansion (~130 K).

4.2.4 Downstream Optical Components

Beam power is no longer an engineering issue downstream of the monochromator. Depending on the application, Kirkpatrick-Baez (KB) mirrors, compound refractive lenses, or zone plates may find focusing application. Micro-focusing optical elements of various types are the subject of intense development work as manifest by the rapidly evolving state of the art.

Rather than try to capture the current state of these developments here, we examine a modest demagnification KB mirror system as a simple means to characterize the PEP-X emittance degradation owing to the upstream optics. We assume the use of a 7:1 horizontal demagnification, *perfect* elliptically figured focusing mirror which focuses at 100 m. This places the mirror 12.5 m upstream of the focus. The horizontal emittance degradation of such an optical system is dominated by the power-filtering mirror system located upstream of the monochromator. Reasonably state-of-the-art mirrors can attain slope errors in the 0.25-µrad rms range (i.e., the hard x-ray offset mirror system used for the LCLS). Assuming an anti-parallel, variable cutoff power-filtering mirror system with two flat mirrors, the effective figure error for the composite system will be √2 larger or 0.35 µrad rms. The point-spread function for this system is ~9 µm rms. In contrast, the ideal demagnified source image is 5.2 µm rms. Consequently, the net horizontal emittance degradation is approximately 1.7-fold. This does not describe the entire beam degradation situation since wavefront-distortion effects are not considered. Applying the Maréchal Criterion for wavefront distortion limits the acceptable distortion to λ/14, which, for a two-mirror system, constrains the mirror surface long-wavelength height variation to λ/(28α√2) rms where α is the beam's incident angle on the mirror surface. Assuming 10-keV radiation and 2.7-mrad incident angle yields a mirror surface height control of 12 Å rms. This limitation is about two times more aggressive than mirror vendors currently find

acceptable. A looser 20-Å rms height error specification results in 50% beam intensity reduction of the coherent beam fraction.

Vertical emittance degradation associated with the upstream (i.e., non-focusing) optics is dominated by the monochromator thermal distortion as discussed above. The degradation is energy-dependent owing both to the energy dependence of the monochromator distortion and the energy dependence of the effective source emittance when the diffraction-limited photon phase space is added in quadrature with the electron source phase space. Quantitative prediction of the vertical emittance degradation awaits a more complete study of the monochromator's thermal response to PEP-X power conditions. It is clear, however, that improved monochromator thermal performance is essential to realizing the full potential of PEP-X.

4.2.5 Beam Line Design Challenges

Given the afore mentioned emittance and phase distortion effects with current beam line technology, it is appropriate to list areas where technological improvements could deliver important beam line cost and/or performance advantages:

- Improved thermal designs could reduce masking costs and provide more beam line layout flexibility.

- Improved mirror cooling technologies couls reduce emittance degradation and improve beam stability.

- Improved mirror polish/figures would reduce emittance and coherence degradation.

- Advanced beam position and shape monitors would enhance beam stability when incorporated into feedback systems.

- Reduced thermal deformation of monochromator crystals through cooling improvements and/or alternative crystals would reduce emittance and coherence degradation as well as improve beam stability. Substantial improvements in power management could eliminate the need for power filtering mirrors. Though not explicitly discussed above, grating monochromators for VUV and soft x-ray beam lines would derive similar benefits from improved thermal performance.

- Advances in micro-focusing optics, such as smaller zone plate line widths, would enhance mircroscope resolution.

- Improvements in optics support and experimental hall floor stability would reduce beam instability.

- Enhancements in permanent magnet and/or superconducting magnet technology could increase source brightness.